

Development and testing of a flexible test bench for high-speed impact shear-cutting with linear motors

Pascal Krutz^{1,a*}, André Leonhardt^{1,b}, Alexander Graf^{1,c}, Sven Winter^{2,d},
Matthias Rehm^{1,e}, Verena Kräusel^{2,f}, Martin Dix^{1,2,g}

¹Institute for Machine Tools and Production Processes, Chemnitz University of Technology,
Reichenhainer Str. 70, Building M, 09126 Chemnitz, Germany

²Fraunhofer Institute for Machine Tools and Forming Technology IWU, Reichenhainer Str. 88,
09126 Chemnitz, Germany

^apascal.krutz@mb.tu-chemnitz.de, ^bandre.leonhardt@mb.tu-chemnitz.de,

^calexander.graf@mb.tu-chemnitz.de, ^dsven.winter@iwu.fraunhofer.de, ^ematthias.rehm@mb.tu-chemnitz.de, ^fverena.kraeusel@iwu.fraunhofer.de, ^gmartin.dix@mb.tu-chemnitz.de

Keywords: Linear Motor, Blanking, High-Speed Impact Shear-Cutting

Abstract. Due to the use of high-strength steels to achieve lightweight construction goals, conventional shear cutting processes are reaching their limits. Therefore, so-called high-speed impact cutting (HSIC) is used to achieve the required cut surface qualities. A new machine concept consisting of linear motors and an impact mass is presented to investigate HSIC. It allows all relevant parameters to be flexibly adjusted and measured. The design and construction of the test bench are described. The validation was performed with HSIC of a mild deep-drawing steel sheet. The velocities as well as the cut surface were analysed.

Introduction

The manufacturing of complex components and assemblies, such as vehicle bodies, requires additional punching operations after the actual forming process in order to be able to realize the final component geometry. On the one hand, this includes the trimming of formed parts, and on the other hand, holes or forming contours are cut into the component to ensure further processing as well as the function of the component. Therefore, a primary challenge is to ensure the required cut quality. Due to the growing importance of lightweight construction, higher, high-strength and ultra-high-strength steels are increasingly being used in vehicle construction [1], which means that the application limits of conventional shear-cutting operations are being reached. One approach to optimize the shear-cutting of ultra-high-strength steels is to exploit high-speed effects in cutting processes. In recent years, the potential of high velocities ($v \geq 10$ m/s) in shear-cutting has been investigated, analysed and evaluated within the framework of various research projects [2–4]. In so-called high-speed impact cutting (HSIC), the early shear failure in the material is exploited by generating adiabatic shear bands [5]. Due to this effect, even ultra-high-strength steels can be cut with a particularly high quality of the cut surfaces in a resource- and energy-efficient way [6]. The current hydraulic HSIC presses can provide very high impact energies (up to 7000 J) and require a large installation space. However, recent studies show that significantly lower energies are required for cutting. Winter et al. [7] were able to show on the 3 mm thick and hardened steel 22MnB5 that already 250 J impact energy and velocities significantly below 10 m/s are sufficient to produce qualitatively very good cutting surfaces. Due to the fact that significantly lower energies and velocities are sufficient, this allows the use of other more flexible drive concepts with significantly smaller installation space. Conceivable here are electromagnetically accelerated drives, such as that of Linnemann et al. [8]. Therefore, an impact body is accelerated, which provides the impulse for the subsequent shear-cutting. However, the disadvantage is that the

accelerated mass is usually below 5 kg, otherwise the coils and the currents are very large, consequently the energy provided is also very low. Pneumatic [9] or explosively [10] operated drives are also conceivable. If larger masses are to be accelerated, however, they quickly reach their limits. Likewise, the explosive drives are hardly transferable to larger industrial areas. So-called linear motors offer an interesting approach here, because in comparison with conventional drives they can reach higher dynamics due to the lack of mechanical coupling elements [11]. These are mainly used in the areas of handling systems, machine tool and special machine building as well as packaging and assembly systems [12]. Linear motors have a high degree of flexibility, are very compact and can easily accelerate masses significantly above 50 kg to the velocity range relevant for the HSIC ($v > 2$ m/s). Nevertheless, linear actuators are not currently used for HSIC. This study will be the first to use the advantages of a linear actuator for the HSIC.

Conception of the high-speed impact cutting process

The principle of a drop tower was adopted for the implementation of HSIC. A large impact mass (IM) is actively accelerated by a linear motor unit and transfers the impulse as an elastic impact to a smaller, float-mounted mass – the shear-cutting tool. The mass ratio and the physical relationship of the elastic impact result in a higher speed of the tool with mounted cutting punch, which should be in the adiabatic range. Fig. 1 describes the distribution of the different energies and their specific calculation. Initially, the kinetic energy of the IM is available, based on the velocity v_{IM0} of the IM before the impact. After the impact, the kinetic energy of the IM splits into a remaining kinetic energy of the IM and the kinetic energy of the upper part of the cutting tool. The latter is available for the blanking process and is divided into the required cutting energy and an available energy for cutting speed.

The quantity of this available energy finally determines the speed at which the cutting punch moves through the sheet metal strip in theory. The required masses of the IM and cutting tool as well as the required processing speeds are calculable inversely via the theoretically occurring cutting speed. This should be in adiabatic range for the generation of reproducible high-speed cutting effects on the workpiece.

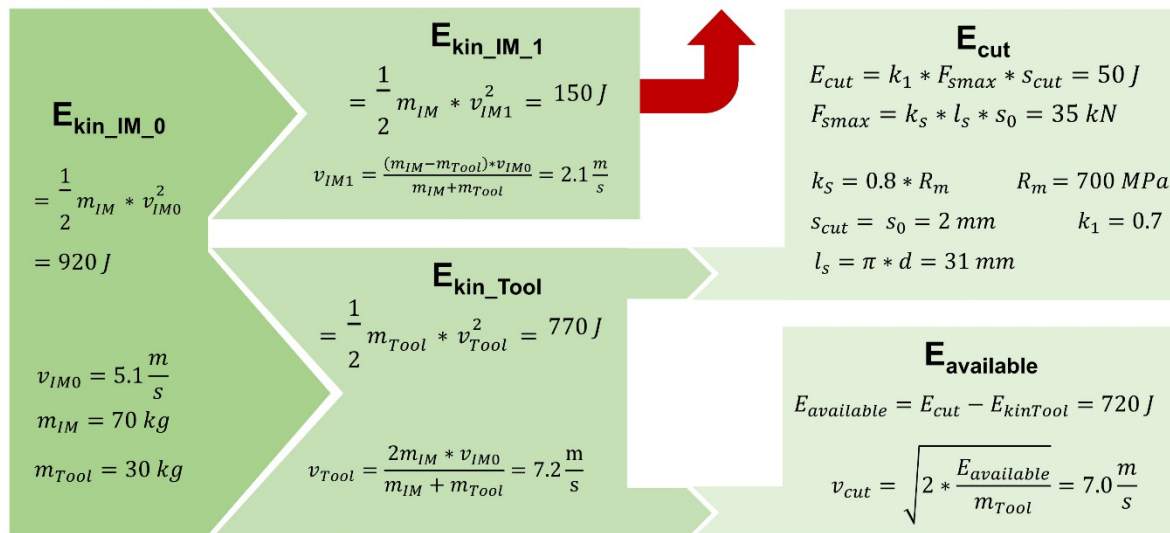


Fig. 1: Allocation of the present process energies for conceptual design and their calculation, assuming an uncoupling speed of the linear motors with 2 m/s

The calculation starts with an impact speed of IM. This is composed of the nominal speed of the linear motors (set to 2.0 m/s) and a residual drop height (assumed to 0.5 m). For the latter, a frictionless acceleration of 9.81 m/s² is assumed for simplification. With these assumptions, the impact velocity v_{IM0} amounts 5.1 m/s. To calculate the velocities of the IM v_{IM1} and the cutting

tool v_{Tool} after the impact, the equations of elastic impact of two masses are used. They are included in an adapted form in Fig. 1. Since the IM has a significantly higher mass than the upper part of the cutting tool, the latter will move at a higher speed than the IM after the impact. In addition to the calculation of the kinetic energies, Fig. 1 also shows the calculation of the cutting energy required for blanking of a sheet metal strip (sheet thickness s_0) with a length of the cutting line l_s . The parameter k_l is a scaling factor in the range 0.4 to 0.7 and k_s describes the shear resistance which can be approximated with $0.8 \cdot$ tensile strength. After calculating the cutting energy and subtracting it from the kinetic energy of the cutting tool after the impact, the remaining amount is used to calculate the theoretical occurring cutting punch speed. In this calculation example, the final cutting speed is around 7 m/s.

Constructive realization of the novel test bench

For practical implementation, a linear motor test bench was considered, which consists of two separately controllable linear motors. They can perform highly dynamic motions up to an acceleration of 100 m/s^2 due to their design and are thus predestined for the acceleration of the IM.

For the integration of the shear-cutting tool into the linear motor test bench, a column guided plate frame was chosen into which the cutting tool was integrated. The plate frame includes a top and base plate, which hold together four cylindrical guide columns with a length of two meters. Two further plates are located between the top and base plates, which can move along the guide pillars with slide bearing sockets. One of these displaceable plates acts as the IM and has to be accelerated by the linear motors. The second movable plate is used for mounting the cutting tool.

The two vertically movable linear motors move synchronously in gantry mode and are connected via an adapter plate. The technical data for the two linear motors from SKF® are specified with maximum force of 3.1 kN each and a maximum feed rate with 7 m/s at nominal force and 2.3 m/s at maximum force. A linking mechanism was constructed on the adapter plate that enables the IM to be picked up. After lifting the IM to the upper end position, the linear motors accelerate downwards at an acceleration greater than the acceleration due to gravity. During this process, the IM is mechanically detached so that the motors decelerate until standstill after reaching the set speed. The detachment of the IM is necessary to protect the motors, as they must not collide with a stationary tool while the IM is linked. After detachment, the IM continues to fall downwards, gaining speed due to gravity.

The cutting tool is provided with an additional mass on the upper side to absorb an increased amount of kinetic energy from the IM during the elastic impact. After the impact of the cutting tool and the IM, the cutting punch immediately performs the shear-cut and the cutting tool subsequently closes by itself. Next, the IM continues to move downwards at a reduced speed and is cushioned by two buffers. Both the cutting tool and the buffers are mounted floating on the so-called assembly table. This table is connected to the frame of the test bench with a spring-damper system in order to transfer the dynamically occurring forces during acceleration and deceleration of the components to a large base area. In Fig. 2, the adapted design of the linear motor test stand is illustrated by comparing it with the concept sketch. Two high-speed cameras were used in combination with two high-power led spotlights to record the process speeds.

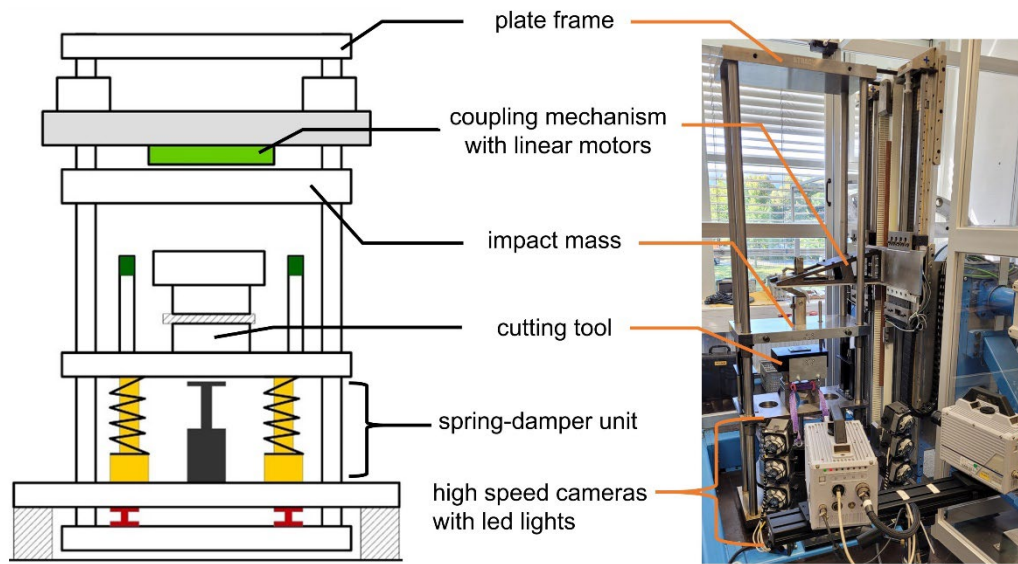


Fig. 2: HSIC test bench - comparison of concept sketch and constructive realisation

In accordance to Fig. 2, the most important requirements for the test stand, their constructive realisation and the resulting specific advantages are summarised in Tab. 1. The main advantage of the test bench is the high flexibility for examination of the HSIC processes, as the applied impact energies can be continuously adjusted and furthermore a good accessibility for the sensory recording of the shear-cutting process is guaranteed.

Tab. 1: Description of technological requirements, the corresponding constructive realisations and derivation of specific advantages

Technological requirement	Constructive/technological implementation
highly dynamic acceleration of the cutting punch	principle of elastic impact, acceleration of an impact mass with linear motors
central localized impact on cutting tool	selection of a frame with column guided plates, one plate is impact mass
variation of the cutting energy	flexible adjustment of the motor dynamics by setting control parameters, optional variation of impact mass and additional tool masses
controlled absorption of dynamic forces	use of a spring-damper system which absorbs impact energy and transfers it to the frame over a large area
linear motors must not collide with stationary masses	construction of a coupling mechanism which enables the automated pick-up and uncoupling of the impact mass
Technological advantages compared to other test benches:	
<ul style="list-style-type: none"> • Precise adjustment of impact energy by adjusting engine dynamics (speed, acceleration, jerk, setting of launch position) and variation of impact and cutting tool masses • High accessibility for sensory acquisition of the HSIC process • Recording of the cutting punch speed with high-speed cameras as no obscuring of the field of vision by enclosures etc. • Integrated motor measuring system enables feedback on the applied impact energy • Easy access to the cutting tool simplifies workpiece handling 	

In the following, the implemented automation and the technological sequence, shown in Fig. 3, are described in more detail. At the beginning, the linear motors are in the start position. Here, the

IM is located on the cutting tool in the uncoupled state. First, the linear motors move down to the IM and pick it up via a fully mechanical coupling mechanism. Afterwards, the IM is lifted by a few centimetres, while the upper part of the cutting tool, including the blank holder, is also lifted. This motion opens the cutting tool and the sheet metal strip can be inserted. Subsequently, the cutting tool is closed and the IM is lifted to the upper end position of the linear motors. With release by the user, the IM is accelerated up to the parametrized uncoupling speed. After uncoupling of IM, it is further accelerated due to gravity until the elastic impact with the tool and the execution of the cutting process. After performing the shear-cutting operation and decelerating the moving masses with the spring-damper unit one cycle is completed.

A pulse-like change in speed of the IM and cutting tool occurs during the cutting process at the beginning of section C in Fig. 3. The speed of the cutting tool adjusts to the cutting speed, which results after the deduction of the required cutting energy. During the cutting process, the cutting punch moves faster through the metal strip than the IM falls at its residual speed. As a result, the cutting tool speed is temporarily at 0 m/s after the cutting process has been completed. As soon as the IM hits the buffers, both IM and cutting tool move downwards at the same speed and are decelerated by the spring-damper unit until they come to a standstill. The realized test bench is characterized in particular by its high flexibility on the part of the process parameters. In addition to the dynamic parameters like jerk, acceleration and velocity of the linear motors, the IM and tool masses can also be adjusted. This results in a fine granular setting of the inserted impact energy.

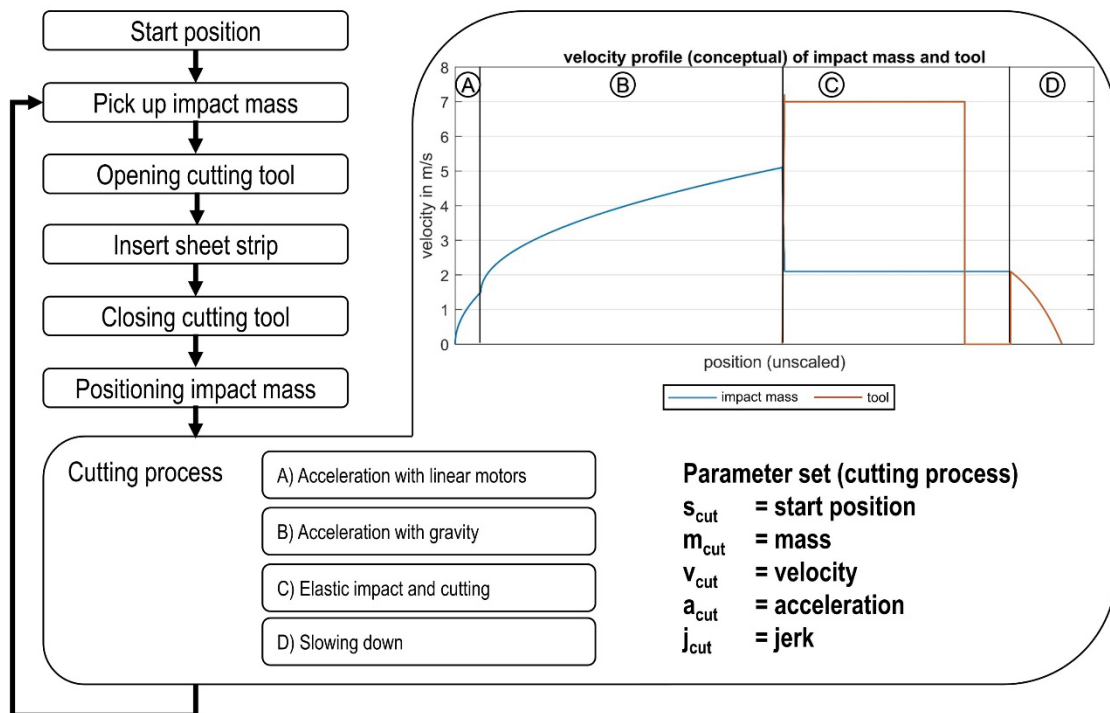


Fig. 3: Technological flowchart for the implementation of HSIC trials

Validation of test bench

After the successful commissioning of the test bench, the functionality of the conceptualised kinematics has to be proven. This includes in particular the effective coupling and decoupling of the IM for different process speeds. Two high-speed cameras were used to determine the process speeds of the IM and the tool. Fig. 4 shows the determined velocity curves of the IM for a motor velocity set to 2.0 m/s. Since the entire movement range cannot be captured with one measuring range of the camera, three relevant measuring ranges, each covering 130 mm in the vertical direction, were selected. The arrangement of the first two upper windows was selected in a way

that, starting with the acceleration of IM from standstill, its speed was recorded approximately continuously over 260 mm. The set speed of the motors was already reached in the first window, with the result that only the acceleration due to gravity is shown in the second window. After passing out of the second window, IM continues to move downwards and is recorded with the third window subsequent at impact height. The intermediary speed curve is linearly interpolated according to the assumption of a uniform acceleration and constant friction and is shown with an interruption for better display of the subsequent camera window in Fig. 4. Window 3 shows a first maximum speed of the tool with approximately 3 m/s, indicating that the adiabatic cutting range has been reached. With 3.5 m/s, the impact velocity of IM is around 1.6 m/s below the theoretically calculated impact velocity v_{IM0} in Fig. 1. The main reasons for this are the frictional forces acting during the acceleration of IM. These were not considered in the conception. If the calculation of the cutting speed is repeated with the measured impact speed, the result is 4.5 m/s for v_{cut} . This implies that v_{cut} is still 1.5 m/s below the calculated speed. This deviation can be partly explained due to a not loss-free energy transfer during the elastic impact. In particular, the floating mounting of the tool contributes to the absorption of parts of the kinetic energy by IM from the spring-damper system. With a good approximation, the new calculated velocity v_{IMI} of 1.4 m/s agrees with the practically measured velocity of IM after the impact. As another cause for deviations, the multiple rebound of IM after the first impact can be mentioned, which means that the highly simplified assumptions for the calculation are only valid to a limited extent.

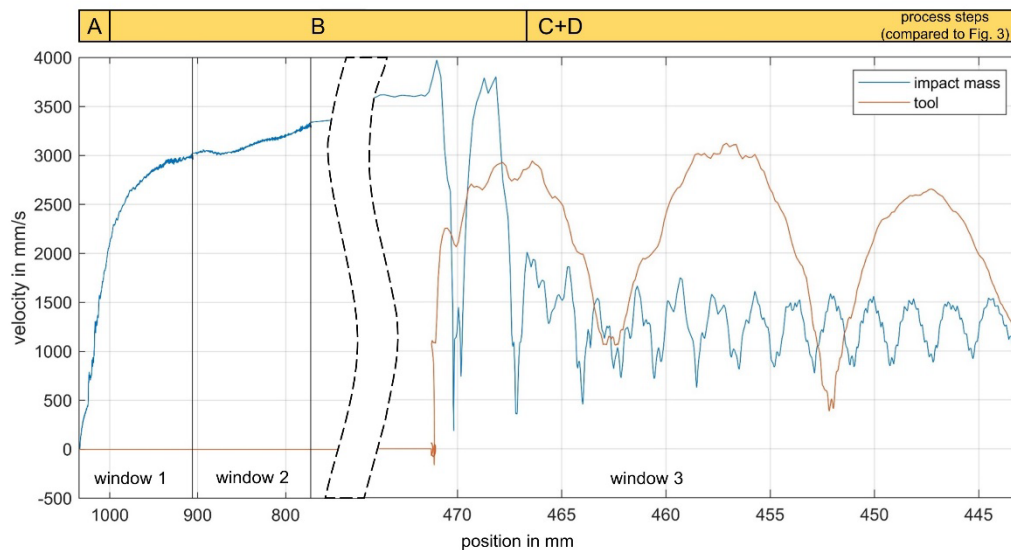


Fig. 4: Measured velocity profile of IM and tool, captured with three different recording windows, consisting of acceleration with linear motors (A), acceleration by free fall (B) and impact with the tool for a set uncoupling speed of 2 m/s (C+D)

Validation of the HSIC process

To validate the flexible test bench, circular blanks with a diameter of 10 mm were cut out of mild deep-drawing steel (1.0338). The fixed parameters for the test series were the sheet thickness ($s = 2$ mm), the related cutting gap ($u_s = 2.5$ %s) and the material mentioned above. The only variation during the validation was the cutting speed. These were three speeds for the uncoupling of IM (1.0, 1.5 and 2.0 m/s) and were supplemented by conventional cutting tests at 0.025 m/s. The first step was the evaluation of the cut surface quality according to VDI 2906 sheet 2 [13]. The summary of the results is shown in the Fig. 5. It can be clearly seen that the roll-over is reduced with increasing cutting speed. On the other hand, the proportion clean-cut zone is reduced and, consequently, the proportion of fracture zone increases with increasing cutting speed. Another positive aspect is the increase in the fracture surface angle when using HSIC. All results have a drastic change from $v =$

0.025 m/s to $v = 2.4$ m/s in common, but a saturation or even a reversal of the results occurs with further increase of the cutting speed.

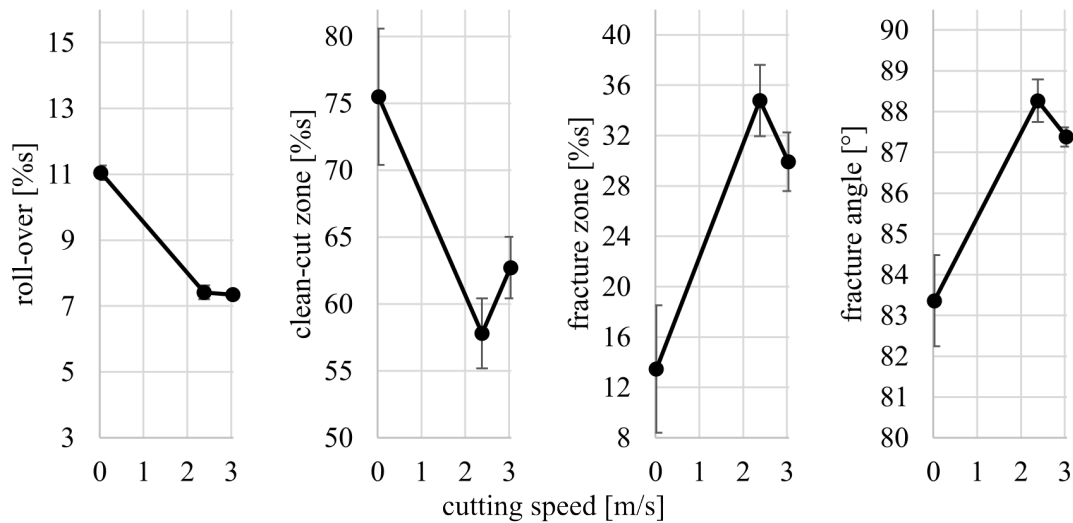


Fig. 5: Influence of the cutting speed on the cutting surface characteristics

With the characterisation of the microstructure by mapping the hardness, further influences of the punch velocity become apparent. At a punch speed of 0.025 m/s, an increasing hardening towards the cut edge is visible (Fig. 6 a). The hardening depth is up to 0.5 mm from the cutting edge. By increasing the punch speed to 3 m/s, the hardening depth decreases to 0.3 mm (Fig. 6 b). It is noticeable that there is a smaller increase in hardness compared to the punch speed of 0.025 m/s in the area from the roll-over up to the beginning of the fracture zone. Observing the microstructure (Fig. 6 c), it becomes clear that a large deformation has occurred in this area. This indicates an adiabatic shear band in this area.

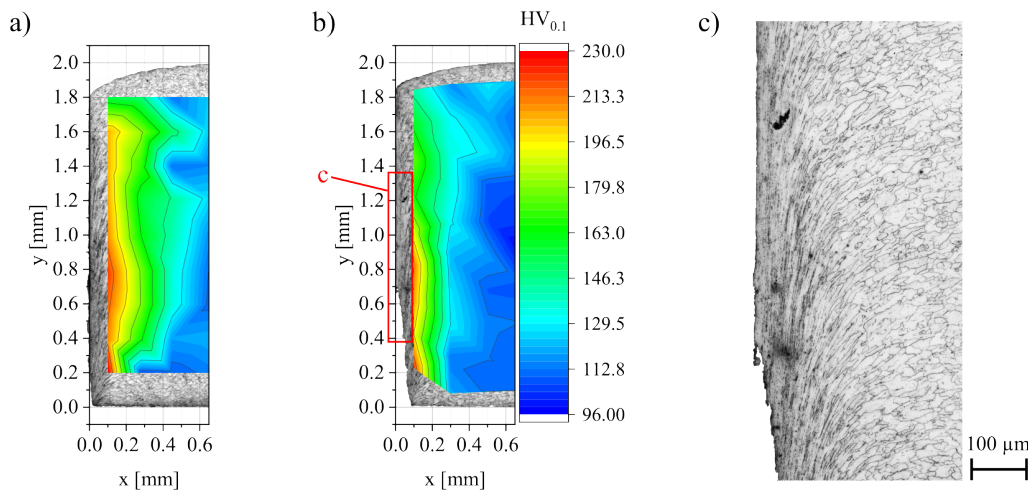


Fig. 6: Measured hardening profiles under variation of the punch speed: a) 0.025 m/s, b) 3 m/s and c) the enlargement of the microstructure in the area of large deformation at 3 m/s

Summary and outlook

HSIC tests were carried out with the presented test bench. Linear motors were used to generate the cutting energy. The construction, which is easily accessible for sensor technology, enabled the precise measuring of occurring tool velocities. Three different decoupling velocities (1.0, 1.5 and 2.0 m/s) were investigated for a mild deep-drawing steel. The determined IM and tool velocities were lower than the conceptually calculated velocities, which is mainly due to the neglect of

frictional forces and energy losses during impact. In the verification of the cutting results, the high punch speed (up to 3 m/s) was proven. This is reflected in the influence on the quality of the cut surface and the microstructure. In the continuation of the presented investigations, the speed of the falling mass is to be further increased, with a main focus on the reduction of friction on guide columns. To further expand the process, it is also planned to cut other materials such as high-strength steels.

References

- [1] Merklein, M.; Wieland, M.; Lechner, M.; Bruschi, S.; Ghiotti, A. Hot Stamping of Boron Steel Sheets with Tailored Properties: A Review. *J. Mater. Process. Technol.* 2016, 228, pp. 11–24. <https://doi.org/10.1016/j.jmatprotec.2015.09.023>
- [2] Hu, D.; Chen, M.; Wang, L.; Wang, H. Microstructural Characterization of Blanked Surface of C5191 Phosphor Bronze Sheet under Ultra-High-Speed Blanking. *Trans. Nonferrous Met. Soc. China* 2021, 31, pp. 692–702. [https://doi.org/10.1016/S1003-6326\(21\)65530-9](https://doi.org/10.1016/S1003-6326(21)65530-9)
- [3] Gaudillière, C.; Ranc, N.; Larue, A.; Lorong, P. Investigations in High Speed Blanking: Cutting Forces and Microscopic Observations. *EPJ Web Conf.* 2010, 6. <https://doi.org/10.1051/epjconf/20100619003>
- [4] Winter, S.; Schmitz, F.; Clausmeyer, T.; Tekkaya, A.E.; Wagner, M.F.X. High Temperature and Dynamic Testing of AHSS for an Analytical Description of the Adiabatic Cutting Process. *IOP Conf. Ser. Mater. Sci. Eng.* 2017, 181. <https://doi.org/10.1088/1757-899X/181/1/012026>
- [5] Rittel, D.; Wang, Z.G.; Merzer, M. Adiabatic Shear Failure and Dynamic Stored Energy of Cold Work. *Phys. Rev. Lett.* 2006, 96. <https://doi.org/10.1103/PhysRevLett.96.075502>
- [6] Schmitz, F.; Winter, S.; Clausmeyer, T.; Wagner, M.F.-X.; Tekkaya, A.E. Adiabatic Blanking of Advanced High-Strength Steels. *CIRP Ann.* 2020, 69, pp. 269–272. <https://doi.org/10.1016/j.cirp.2020.03.007>
- [7] Winter, S.; Nestler, M.; Galiev, E.; Hartmann, F.; Psyk, V.; Kräusel, V.; Dix, M. Adiabatic Blanking: Influence of Clearance, Impact Energy, and Velocity on the Blanked Surface. *J. Manuf. Mater. Process.* 2021, 5, 35. <https://doi.org/10.3390/jmmp5020035>
- [8] Linnemann, M.; Scheffler, C.; Psyk, V. Numerically Assisted Design For Electromagnetically Driven Tools. *Procedia Manuf.* 2020, 47, pp. 1334–1338. <https://doi.org/10.1016/j.promfg.2020.04.254>
- [9] Yaldız, S.; Sağlam, H.; Ünsaçar, F.; Işık, H. Design and Applications of a Pneumatic Accelerator for High Speed Punching. *Mater. Des.* 2007, 28, pp. 889–896. <https://doi.org/10.1016/j.matdes.2005.10.009>
- [10] Mottram, A.R. High Energy Rate Forming Techniques. In *Mechanical Engineer's Reference Book*; Elsevier, 1973. <https://doi.org/10.1016/B978-0-408-00083-3.50022-9>
- [11] Rehm, M.; Quellmalz, J.; Schlegel, H.; Neugebauer, R. Control Strategies for Mechanically-Coupled High Speed Linear Drives. In *Proceedings of the Proceedings of the Ninth International Symposium on Linear Drives for Industry Applications*; Hangzhou, 2013; pp. 273–278.
- [12] Bernstein, H. Gleichstrom-, Schritt- Und Linearmotoren. In *Elektrotechnik/Elektronik für Maschinenbauer*; Springer Fachmedien Wiesbaden: Wiesbaden, 2018; pp. 289–329. https://doi.org/10.1007/978-3-658-20838-7_6
- [13] VDI 2906 Blatt 2- Schnittflächenqualität beim Schneiden - Scherschneiden 1994.